

Atomic Rydberg-state excitation in strong spatially inhomogeneous fieldsShilin Hu,^{1,*} Xiaopeng Yi,² Li Guo,³ Chengrui Bi,² and Jing Chen^{4,5,†}¹*Guangdong Provincial Key Laboratory of Quantum Metrology and Sensing & School of Physics and Astronomy, Sun Yat-Sen University (Zhuhai Campus), Zhuhai 519082, China*²*Institute of Applied Physics and Computational Mathematics, P. O. Box 8090, Beijing, 100088, China*³*Department of Physics, Shanghai Normal University, Shanghai 200234, China*⁴*Department of Modern Physics, and Hefei National Research Center for Physical Sciences at the Microscale and School of Physical Sciences, University of Science and Technology of China, Hefei 230026, China*⁵*Shenzhen Key Laboratory of Ultraintense Laser and Advanced Material Technology, Center for Advanced Material Diagnostic Technology, and College of Engineering Physics, Shenzhen Technology University, Shenzhen 518118, China*

(Received 5 October 2022; revised 6 January 2023; accepted 16 February 2023; published 7 March 2023)

We investigated the Rydberg-state excitation process of a hydrogen atom subjected to spatially homogeneous and inhomogeneous laser fields by means of *ab initio* calculations. It is found that, comparing with atoms exposed to spatially homogeneous laser fields, the excitation probability decreases and the electron tends to occupy the states with lower principal quantum numbers and angular quantum numbers for atoms in spatially inhomogeneous laser pulses. Furthermore, calculations of a quantum model without taking into account ionization of the electron after it is coherently captured by the Rydberg state are inconsistent with the above-stated findings by *ab initio* calculations. Analysis indicates that the aforementioned intriguing features can be attributed to the enhanced ionization of the Rydberg states by inhomogeneous laser fields since the distributions of Rydberg states of high principal quantum numbers and angular quantum numbers locate far away from the core where the inhomogeneous electric fields become significant.

DOI: [10.1103/PhysRevA.107.033104](https://doi.org/10.1103/PhysRevA.107.033104)**I. INTRODUCTION**

Generations of Rydberg-state atoms and molecules subjected to intense laser pulses have gained significant attention in the past decade since high-lying Rydberg-state atoms and molecules can be explored to investigate quantum phenomena and provide novel quantum objects of mesoscopic size for probing classical-quantum correspondence [1–3]. Such atoms and molecules have important applications in the fields of quantum information [4], precision measurements [5], and acceleration and deceleration of neutral samples [6–8]. In addition, the manipulations of electrons in Rydberg-state atoms and molecules are helpful for controlling chemical reactions [9] and understanding the physical mechanisms of the photoelectron spectral features and below-threshold harmonic generation of atoms exposed to intense laser pulses [10,11].

In experiments, Rydberg-state excitation (RSE) has been detected in atoms and atomic fragments produced from Coulomb explosion of molecules in intense laser pulses [12–21]. A model of interference stabilization (IS) has been put forward to explain the generation of Rydberg-state samples and the physical reason of interference stabilization is ascribed to the interference of the amplitudes of transitions to continuum from the excited Rydberg states, which are coherently repopulated by the Raman transitions for atoms and molecules subjected to laser pulses [22–26]. Another model

of frustrated tunneling ionization (FTI) is often employed to interpret the formation of neutral species in intense laser fields [13,27] in which electrons are driven by the laser field after tunneling through the potential barrier formed by the combined Coulomb and laser fields and a fraction of them are trapped into highly excited states due to the Coulomb field of the parent core after the laser pulse is switched off. The aforementioned FTI mechanism is actually the same picture of recapture put forward to explain the generation of Rydberg atoms exposed to strong laser pulses [28]. For the theoretical calculations by numerically solving time-dependent Schrödinger equations, the generation of Rydberg atoms and peak structures of intensity-dependent Rydberg-state populations in intense laser fields are ascribed to the mechanisms of the Freeman-resonance perspective and the continuation of above-threshold ionization (ATI) to the below-threshold negative energy region [29–31].

Recently, a quantum model (QM) was proposed to interpret the formation of Rydberg atoms as a coherent recapture process accompanying by the ATI process [32]. In the aforementioned quantum model [32], the electron is first promoted to the continuum by the laser field, it subsequently evolves in the external field, and a fraction of the electrons may be coherently captured into Rydberg states during the laser pulse, which is different from the above IS and FTI models. In the quantum model, the ionization process of the Rydberg-state atom is not taken into account since the ionization of the Rydberg state is small due to stabilization [31]. The physical picture of the quantum model is similar to that of IS and the electron transits from the continuum state to

*hushlin@mail.sysu.edu.cn

†chenjing@ustc.edu.cn

the Rydberg states after the transition from the ground state to the continuum state in both models, so the physical process in the quantum model can be considered as a generalized Raman process. More recently, the quantum model was extended to study atomic Rydberg-state excitation subjected to laser pulses of long wavelengths [33].

Previous investigations of atomic RSE process mainly focused on the spatially homogeneous laser fields. Recently, the features of intense-field ionization and harmonic spectra for atoms subjected to spatially inhomogeneous fields attracted considerable attentions [34–41]. The harmonic intensity in the plateau region can be significantly enhanced and a broadband xuv continuum can be generated for the hydrogen atom exposed to spatially inhomogeneous fields [42]. It is found that the inhomogeneity of the enhanced plasmonic field has an important impact on the ATI process and high-energy electrons with energies in the near-keV regime can be produced for the atom subjected to inhomogeneous fields [43]. Recently, it was demonstrated that the returning energy of the rescattering electron is enormously increased and the time window of tunneling ionization where the electron can be driven back to generate photoelectron holography is evidently broadened for the hydrogen atom in the spatially inhomogeneous fields [44].

As stated above, the characteristics of atomic ionization and harmonic spectroscopy in spatially inhomogeneous fields were investigated extensively and the atomic RSE process is closely related to atomic ionization [13,28,32]. The Rydberg-state electron is far away from the parent ion where the inhomogeneous laser fields become evident, so the features of atomic RSE process by intense inhomogeneous laser pulses is an intriguing problem. In addition, it is a question of interest to utilize the recently proposed quantum model to study atomic RSE in strong nonhomogeneous laser fields. In the present work, we investigated the RSE process of hydrogen atom exposed to inhomogeneous laser fields and found that the excitation yields and the spatial distribution of Rydberg states are sensitive to the strengths of the inhomogeneous laser fields due to the ionization of the Rydberg-state atom by laser fields. Atomic units (a.u.) are utilized unless otherwise indicated.

II. THEORETICAL CALCULATIONS

A. Time-dependent Schrödinger equation

The interactions between hydrogen atom and intense laser fields can be modeled by numerically performing the full-dimensional time-dependent Schrödinger equation (TDSE) calculations in the length gauge [44–46]

$$i \frac{\partial}{\partial t} \Psi(\mathbf{r}, t) = \left[-\frac{1}{2} \nabla^2 - \frac{1}{r} + V_{\text{laser}}(\mathbf{r}, t) \right] \Psi(\mathbf{r}, t). \quad (1)$$

The potential $V_{\text{laser}}(\mathbf{r}, t)$ indicates the interaction of the atomic electron and the laser field and the field is assumed to be linearly polarized along the z axis. Due to the spatial dependence of the laser field, it has the following formula:

$$V_{\text{laser}}(\mathbf{r}, t) = E_0 \sin^2(\pi t/t_{\text{max}}) \sin(\omega t) z (1 + \beta z), \quad (2)$$

where E_0 , t_{max} , and ω denote the maximum electric field, the duration, and the frequency of the laser pulse, respectively,

and β is a small parameter which characterizes the inhomogeneity of the laser field. For the Rydberg-state atom of the principal quantum number $n = 10$, the parameter βr is around 0.3 with $\beta = 0.003$ a.u., so the field is strong spatially inhomogeneous in atomic scale.

The time-varying wave function is expanded in terms of B-splines and spherical harmonics as

$$\Psi(\mathbf{r}, t) = \sum_{\mu lm} C_{\mu lm}(t) \frac{B_{\mu}^k(r)}{r} Y_{lm}(\theta, \phi), \quad (3)$$

where $k = 7$ indicates the order of B-splines [45,47]. The target atom is in the ground state ($1s$) and the magnetic quantum number is a good quantum number, so we take the magnetic quantum number $m = 0$. The aforementioned time-dependent wave function is evolved by the Crank-Nicolson scheme [45,47] and a $\cos^{1/4}$ absorber function is employed near the boundary to avoid unphysical reflection of electronic wave functions. The Rydberg-state probability is calculated by projecting the wave function onto the corresponding field-free eigenstates after the conclusion of the strong laser pulse [45,46] and the ionization probability is written as $P_{\text{ion}} = 1 - \sum_n |\langle \psi_n(\mathbf{r}) | \Psi(\mathbf{r}, t_{\text{max}}) \rangle|^2$, where ψ_n indicates the bound state calculated by a diagonalization scheme of the field-free Hamiltonian matrix.

In the present work, the truncated radius is $r_{\text{max}} = 1000$ a.u., 1100 B-splines are employed for the radial wave function, and the maximum number of partial waves is $L_{\text{max}} = 80$. The hydrogen atom ($1s$) is exposed to eight-cycle laser pulses of frequency $\omega = 0.057$ a.u. ($\lambda = 800$ nm), and the time step is $\Delta t = 0.03$ a.u. Convergence of numerical calculations is reached with the above settings.

B. Quantum model

The Rydberg-state excitation of the hydrogen atom in strong, spatially inhomogeneous fields is also examined by the quantum model put forward recently, and the transition amplitude reads as [32]

$$M_{nlm} = (-i)^2 \int_{-\infty}^{\infty} dt \int_{-\infty}^t dt' \int d^3\mathbf{p} \langle \Psi_{nlm}^d(t) | V(\mathbf{r}) | \Psi_{\mathbf{p}}^{(V)}(t) \rangle \times \langle \Psi_{\mathbf{p}}^{(V)}(t') | H_I(\mathbf{r}', t') | \Psi_g(t') \rangle, \quad (4)$$

where t' and t represent ionization and capture times, respectively. $\Psi_g(\mathbf{r}, t) = e^{iI_p t} \psi_g(\mathbf{r})$ denotes the field-free ground state possessing the ionization energy I_p , and the inhomogeneous field-atom interaction is $H_I(\mathbf{r}', t') = \int^{t'} E(\mathbf{r}, t') d\mathbf{r}$. $|\Psi_{\mathbf{p}}^{(V)}(t)\rangle$ represents the Volkov state with asymptotic momentum \mathbf{p} in the length gauge

$$|\Psi_{\mathbf{p}}^{(V)}(t)\rangle = \frac{1}{(2\pi)^{3/2}} \exp \left\{ i[\mathbf{p} + \mathbf{A}(\mathbf{r}, t)] \cdot \mathbf{r} - \frac{i}{2} \int^t dt' [\mathbf{p} + \mathbf{A}(\mathbf{r}, t')]^2 \right\}. \quad (5)$$

The field-dressed Rydberg state is expressed as $|\Psi_{nlm}^d(t)\rangle = \psi_{nlm}(\mathbf{r}) e^{-iE_n t} e^{i\mathbf{A}(\mathbf{r}, t) \cdot \mathbf{r}} e^{-i \int_{-\infty}^t d\tau A^2(\mathbf{r}, \tau)/2}$, where $\psi_{nlm}(\mathbf{r})$ represents a field-free Rydberg state of the hydrogen atom, which possesses the principal quantum number n , angular quantum

number l , and magnetic quantum number m , and the Coulomb potential is $V(r) = -1/r$.

Since the distribution of the ground state of the hydrogen atom is localized, the vector potential and the electric field are assumed to be spatially homogeneous for the electron transition from the ground state to continuum states in Eq. (4). Equation (4) is given by

$$M_{nlm} = (-i)^2 \int_{-\infty}^{\infty} dt \int_{-\infty}^t dt' \int d^3\mathbf{p} V_{nlm,\mathbf{p}} V_{\mathbf{p}g} \exp[iS_n(t, t', \mathbf{p})], \quad (6)$$

where

$$V_{nlm,\mathbf{p}} = \frac{1}{(2\pi)^{3/2}} \int d^3\mathbf{r} \psi_{nlm}^*(\mathbf{r}) \frac{\exp(i\mathbf{p} \cdot \mathbf{r})}{r} \times \exp\left[-\frac{i}{2} \int^t d\tau [\mathbf{p} \cdot \mathbf{A}(\mathbf{r}, \tau) + \mathbf{A}(\mathbf{r}, \tau) \cdot \mathbf{p}]\right], \quad (7)$$

$$V_{\mathbf{p}g} = \frac{1}{(2\pi)^{3/2}} \int d^3\mathbf{r}' \exp[-i[\mathbf{p} + \mathbf{A}(t')] \cdot \mathbf{r}'] \mathbf{r}' \cdot \mathbf{E}(t') \psi_g(\mathbf{r}'), \quad (8)$$

and the action is

$$S_n(t, t', \mathbf{p}) = -\frac{1}{2} \mathbf{p}^2 (t - t') + E_n t + I_p t' + \frac{1}{2} \int_{t'}^t d\tau [A^2(\tau) + 2\mathbf{p} \cdot \mathbf{A}(\tau)]. \quad (9)$$

Here the electric field is given by $\mathbf{E}(\mathbf{r}, t) = E_0 \sin^2(\pi t/t_{\max}) \sin(\omega t) (1 + 2\beta z) \hat{e}_z$ with unit vector \hat{e}_z , and the vector potential is defined as $\mathbf{A}(\mathbf{r}, t) = -\int_0^t \mathbf{E}(\mathbf{r}, t') dt'$. E_0 , ω , t_{\max} , and $E_n = -1/(2n^2)$ represent the laser electric field amplitude, the central frequency, the duration, and the Rydberg-state energy level, respectively. The integration over \mathbf{p} is obtained by the saddle-point method and numerical integrations over the recapture time t and the ionization time t' are performed. The probability of the n th Rydberg state is defined as $P_n = \sum_{l,m} |M_{nlm}|^2$ after the laser pulse is switched off. The detailed calculations can be found in our previous work [32].

In our simulations, the target atom (hydrogen) is in its ground state ($1s$), and $1s$ wave function is expressed as $\psi_{1s}(\mathbf{r}') = \frac{1}{\sqrt{\pi}} e^{-r'}$ with the ionization energy $I_p = 0.5$ a.u. In addition, due to the fact that the nonhomogeneous field is linearly polarized, the magnetic quantum number is conserved and consequently we can consider only $m = 0$ in the following simulations. The laser pulse duration is eight optical cycles of the wavelength $\lambda = 800$ nm.

III. RESULTS AND DISCUSSIONS

In Fig. 1, we depict ionization probabilities and excitation probabilities as a function of laser intensities for hydrogen atom in spatially homogeneous and inhomogeneous fields, which are calculated by TDSE simulations. It is demonstrated that excitation probabilities and ionization probabilities show out of phase with increasing laser intensities for $\beta = 0$ a.u., which has been ascribed to the channel closing effect in Ref. [31]. As the inhomogeneity parameter β is increased, the excitation yields tend to decrease while the ionization

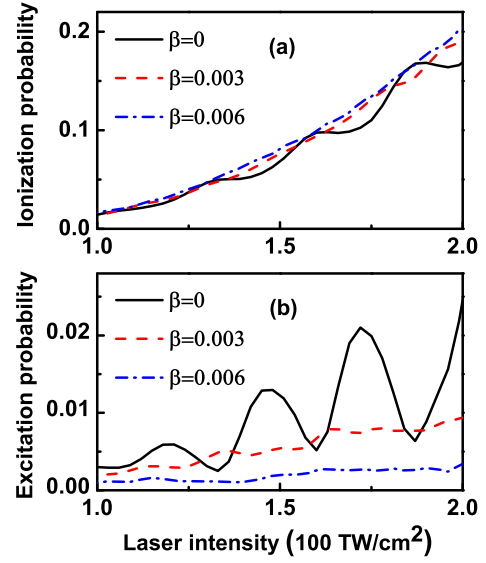


FIG. 1. (a, b) Intensity-dependent ionization and excitation probabilities ($n > 3$) obtained by TDSE simulations for a hydrogen atom exposed to spatially homogeneous and inhomogeneous laser fields (the parameter of β characterizes the inhomogeneity of the laser field and the value of β is given in atomic units).

probabilities tend to increase, which will be discussed further in the following sections.

To shed more insights on the above intriguing behavior of atomic excitation versus the inhomogeneity parameter β , we plot the distributions of the Rydberg-state electrons over different principal quantum numbers for the hydrogen atom in the presence of spatially homogeneous and inhomogeneous laser fields at 172 TW/cm² and 196 TW/cm² in Fig. 2, which are obtained by TDSE calculations. It can be seen that the maximum of the RSE shifts from the principal

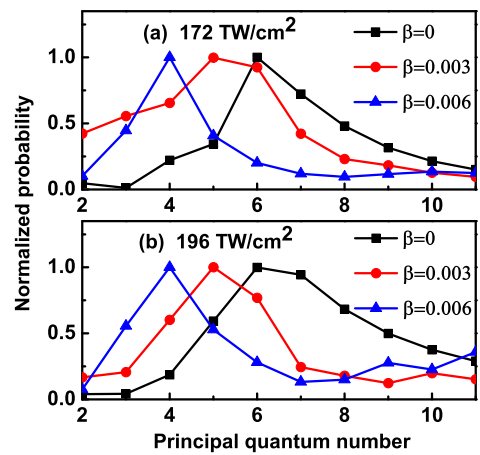


FIG. 2. Distributions of the Rydberg-state electrons over principal quantum numbers calculated by TDSE simulations for the hydrogen atom subjected to spatially homogeneous and inhomogeneous laser fields with different peak laser intensities: (a) 172 TW/cm² and (b) 196 TW/cm². Normalized probabilities are shown for visual convenience and the value of β is given in atomic units.

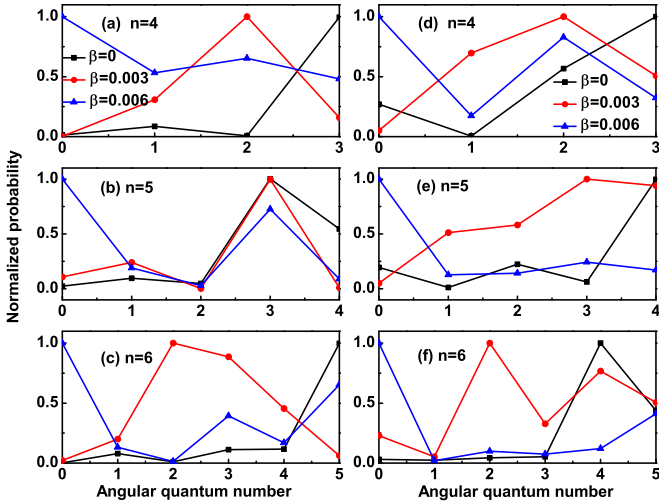


FIG. 3. Distributions of the Rydberg-state electrons over angular quantum numbers of a specific principal quantum number obtained by TDSE calculations for the hydrogen atom exposed to spatially homogeneous and inhomogeneous fields with different laser intensities. (a)–(c) 172 TW/cm²; (d)–(f) 196 TW/cm². Normalized probabilities are plotted for visual convenience and the value of β is given in atomic units.

quantum number $n = 6$ to $n = 4$ when the inhomogeneity parameter increases from $\beta = 0$ a.u. to $\beta = 0.006$ a.u. for the same laser intensity. Since the peak probability shows up in Rydberg states $n = 4, 5,$ and 6 for different inhomogeneity parameters β at a specific laser intensity, we depict the distributions of the Rydberg-state electrons over the angular quantum numbers obtained by TDSE simulations for a given principal quantum number when the hydrogen atom is subjected to spatially homogeneous and inhomogeneous fields of laser intensities 172 TW/cm² and 196 TW/cm² in Fig. 3. It is demonstrated that the electron tends to occupy the Rydberg state of lower angular quantum number with increasing inhomogeneity parameters β for the principal quantum number $n = 4$ in Fig. 3(a) and analogous phenomena can be found for the electron lying in the Rydberg states of the specific principal quantum number in Figs. 3(b) to 3(f).

To further understand the aforementioned distinct atomic RSE behaviors, QM is also employed to investigate the RSE process for the hydrogen atom exposed to spatially inhomogeneous laser fields. We depict the excitation probabilities versus laser intensities for the hydrogen atom subjected to spatially homogeneous and inhomogeneous fields obtained by QM simulations in Fig. 4(a). It is shown that the variation of the intensity-dependent excitation probability is not obvious with the increasing inhomogeneity parameter in Fig. 4(a), which is evidently different from those obtained by TDSE simulations in Fig. 1(b). We also plot the distributions of the Rydberg-state electrons over principal quantum numbers obtained by QM calculations at 172 TW/cm² and 196 TW/cm² in Figs. 4(b) and 4(c), and find that the n distribution is almost independent of the inhomogeneity parameters for the same laser intensity. In addition, distributions of the Rydberg-state electrons over angular quantum numbers of a given principal quantum number are shown in Fig. 5 for laser intensities of

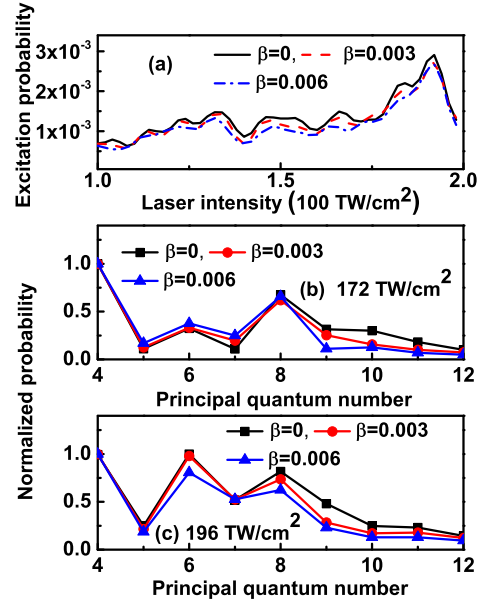


FIG. 4. (a) Excitation probability as a function of laser intensities for different inhomogeneity parameters β by QM calculations ($n > 3$). (b), (c) Distributions of the Rydberg-state electrons over principal quantum numbers calculated by QM simulations at 172 TW/cm² and 196 TW/cm². Normalized probabilities are depicted for comparison and the value of β is given in atomic units.

172 TW/cm² and 196 TW/cm², which are obtained by QM calculations, and the results of $\beta = 0$ a.u. are close to those of $\beta = 0.003$ a.u. and $\beta = 0.006$ a.u. for a specific principal quantum number at the same laser intensity, while the Rydberg-state electron prefers to occupy the state of lower angular quantum number with increasing inhomogeneity

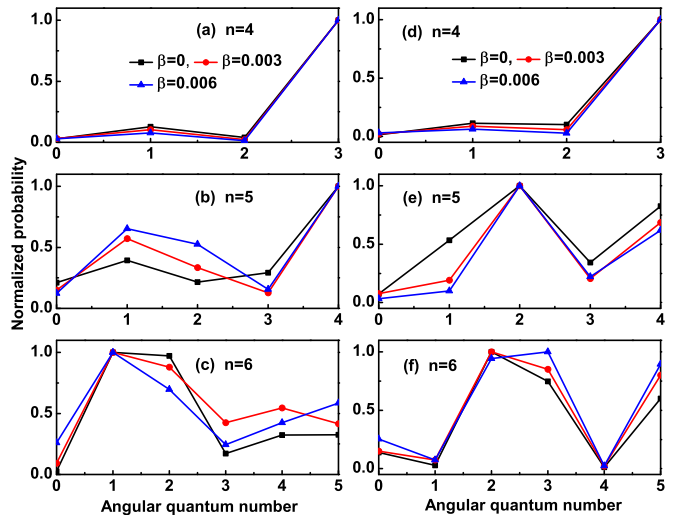


FIG. 5. Distributions of the Rydberg-state electrons over angular quantum numbers of a specific principal quantum number obtained by QM simulations for the hydrogen atom in the presence of spatially homogeneous and inhomogeneous fields possessing different laser intensities. (a)–(c) 172 TW/cm²; (d)–(f) 196 TW/cm². Normalized probabilities are shown for comparison and the value of β is given in atomic units.

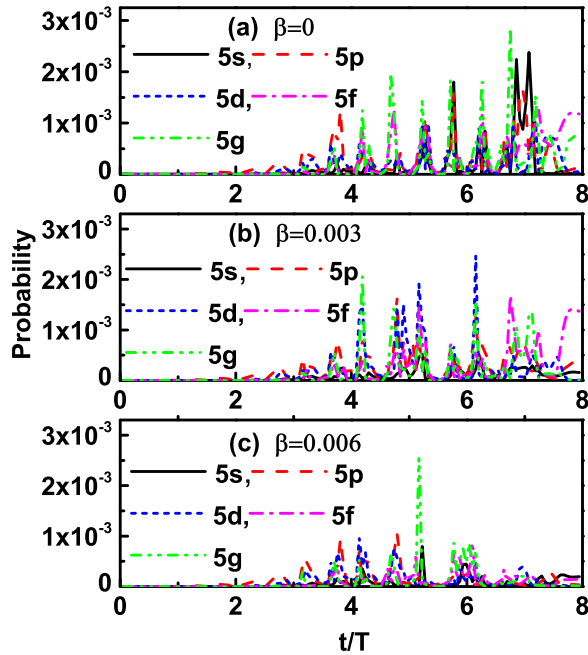


FIG. 6. Time-varying probabilities of excited states with $n = 5$ and different angular quantum numbers obtained by TDSE simulations using initial state $1s$ of hydrogen atom exposed to spatially homogeneous and inhomogeneous laser fields at 172 TW/cm^2 (the value of β is given in atomic units and $T = 2\pi/\omega$).

parameters β for the same principal quantum number at the given laser intensity in Fig. 3. Distributions of the Rydberg-state electrons over principal quantum numbers and angular quantum numbers based on QM simulations in Figs. 4 and 5 are significantly different from those obtained by TDSE calculations in Figs. 2 and 3.

The occurrence of the ionization of the Rydberg-state electron has been neglected in the QM simulations, which was taken into account in TDSE calculations, and the above process may have an important impact on the final formation of the Rydberg-state atom. Since a substantial fraction of the electron occupies the Rydberg state $n = 5$ in Fig. 2, time-dependent probabilities of Rydberg states of $n = 5$ with different angular quantum numbers are plotted in Fig. 6, which are calculated by TDSE simulations for the hydrogen atom subjected to spatially homogeneous and inhomogeneous laser fields at 172 TW/cm^2 . It is shown that the probabilities of Rydberg states of $n = 5$ and different angular quantum numbers become significant after $t = 3T$, and the probabilities of Rydberg states with higher angular quantum numbers decrease significantly with enhancing inhomogeneity parameters β after the laser pulses are switched off. The reason is that the role of inhomogeneous electric fields becomes significant for large z with increasing inhomogeneity parameters β and the distributions of Rydberg states with high angular quantum numbers are far away from the core, therefore, Rydberg-state atoms of high angular quantum numbers are more probable to be detached by the laser fields. As a result, the Rydberg-state electron tends to occupy states with lower principal quantum numbers and angular quantum numbers with increasing β in Figs. 2 and 3. To study the dependence of

TABLE I. Comparison of ionization yields of hydrogen atom using different initial states ($m = 0$) in spatially homogeneous and inhomogeneous laser fields at 172 TW/cm^2 and 196 TW/cm^2 with the duration of four optical cycles based on TDSE simulations.

Initial state	$\beta = 0$ a.u.	$\beta = 0.003$ a.u.	$\beta = 0.006$ a.u.
172 TW/cm^2			
$5s$	0.6561	0.9792	0.9953
$5p$	0.5301	0.9846	0.9939
$5d$	0.6677	0.9847	0.9981
$5f$	0.6083	0.9909	0.9961
$5g$	0.5074	0.9817	0.9976
196 TW/cm^2			
$5s$	0.6941	0.9895	0.9961
$5p$	0.5645	0.9887	0.9973
$5d$	0.6852	0.9939	0.9976
$5f$	0.6521	0.9958	0.9969
$5g$	0.5703	0.9954	0.9993

the ionization behaviors of Rydberg-state atoms on angular quantum numbers, Rydberg states of $n = 5$ with different angular quantum numbers are employed as initial states in the TDSE simulations, and we show the ionization probabilities of the hydrogen atom with different initial states ($m = 0$) subjected to spatially homogeneous and inhomogeneous laser fields at 172 TW/cm^2 and 196 TW/cm^2 with four optical cycles in Table I. It is demonstrated that the ionization yields of Rydberg-state atoms with lower angular quantum numbers are significant compared with that of Rydberg-state atoms with higher angular quantum numbers, especially for the $5g$ state in homogeneous laser fields, while the ionization of hydrogen atom in Rydberg states possessing higher angular quantum numbers, especially for the $5g$ state, gradually becomes evident with respect to that of the hydrogen atom in other states of lower angular quantum numbers with increasing β . Consequently, the ionization process of Rydberg-state atoms plays a vital role in excitation yields and distributions of Rydberg states versus principal quantum numbers and angular quantum numbers for the hydrogen atom in spatially inhomogeneous laser fields.

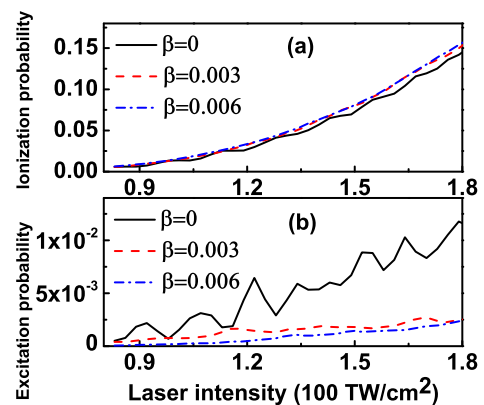


FIG. 7. (a), (b) Same as those in Fig. 1, but for the hydrogen atom exposed to 1000-nm laser fields (the value of β is given in atomic units).

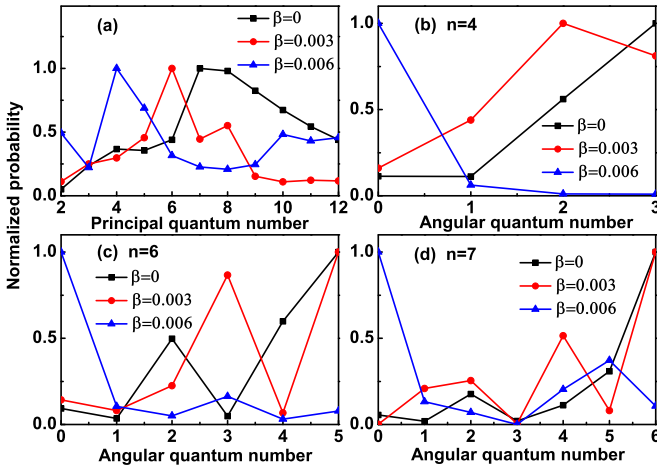


FIG. 8. Distributions of the Rydberg-state electrons over principal quantum number and angular quantum numbers of a given principal quantum number calculated by TDSE simulations for the hydrogen atom subjected to spatially homogeneous and inhomogeneous fields with the laser pulse of the intensity $131 \text{ TW}/\text{cm}^2$ and the wavelength 1000 nm . Normalized probabilities are presented for visual convenience and the value of β is given in atomic units.

In Fig. 7, the ionization probabilities and excitation probabilities as a function of laser intensities are plotted for the hydrogen atom subjected to spatially homogeneous and inhomogeneous laser fields with the wavelength 1000 nm and the aforementioned results are obtained by TDSE calculations. It is also found that the excitation yields tend to decrease while the ionization probabilities tend to increase with the increasing inhomogeneity parameter β , which is similar to those in Fig. 1. In Fig. 8(a), we display the distributions of the Rydberg-state electrons over the principal quantum number for the hydrogen atom exposed to the laser pulses of the peak intensity $131 \text{ TW}/\text{cm}^2$, the wavelength 1000 nm , and different inhomogeneity parameters β , and the electron prefers to occupy the states of lower principal quantum number with increasing inhomogeneity parameter, which is analogous to the results of Fig. 2. Moreover, distributions of the Rydberg-state electrons over angular quantum numbers of a specific

principal quantum number are shown in Figs. 8(b) to 8(d), and the electron tends to occupy the state of lower angular quantum number with increasing inhomogeneity parameter β , which is similar to those of Fig. 3. Consequently, the excitation yields tend to decrease with enhancing inhomogeneous laser fields, which can be ascribed to the enhanced ionization of the Rydberg state by inhomogeneous laser fields since the distributions of the Rydberg state of high principal quantum numbers and angular quantum numbers are far away from the parent ion where the inhomogeneous electric fields become significant. As the inhomogeneity parameter β is increased, the ionization yields tend to increase due to the enhanced ionization of the bound-state electron.

IV. CONCLUSION

In summary, we studied RSE process of the hydrogen atom subjected to spatially inhomogeneous laser fields by TDSE simulations. It is demonstrated that the excitation yields decrease and the Rydberg-state electron prefers to occupy the states of low principal quantum numbers and angular quantum numbers with enhancing spatially inhomogeneous laser fields. In addition, QM calculations are employed to investigate RSE process of hydrogen atom in the presence of spatially inhomogeneous laser pulses and the above-stated TDSE results cannot be reproduced by QM simulations since the occurrence of the ionization process of the electron lying in Rydberg states is neglected in QM calculations. The distributions of Rydberg states with high angular quantum numbers are far away from the parent ion and the impact of electric fields on the ionization of Rydberg-state atoms become evident for large z with enhancing inhomogeneous laser fields, so the above-stated TDSE results are ascribed to the ionization of the electron after it is recaptured by the Rydberg state in spatially inhomogeneous laser fields.

ACKNOWLEDGMENTS

S. L. Hu acknowledges Prof. J. Guo for helpful discussions. This work was supported by the National Basic Research Program of China (Grant No. 2019YFA0307700) and the National Natural Science Foundation of China (Grant No. 12274300).

- [1] T. F. Gallagher, *Rydberg Atoms* (Cambridge University Press, Cambridge, England, 1994).
- [2] F. B. Dunning, J. J. Mestayer, C. O. Reinhold, S. Yoshida, and J. Burgdörfer, Engineering atomic Rydberg states with pulsed electric fields, *J. Phys. B: At. Mol. Opt. Phys.* **42**, 022001 (2009).
- [3] S. Larimian, S. Erattupuzha, C. Lemell, S. H. Yoshida, S. Nagele, R. Maurer, A. Baltuška, J. Burgdörfer, M. Kitzler, and X. H. Xie, Coincidence spectroscopy of high-lying Rydberg states produced in strong laser fields, *Phys. Rev. A* **94**, 033401 (2016).
- [4] M. Saffman, T. G. Walker, and K. Mølmer, Quantum information with Rydberg atoms, *Rev. Mod. Phys.* **82**, 2313 (2010).
- [5] A. Facon, E.-K. Dietsche, D. Grosso, S. Haroche, J.-M. Raimond, M. Brune, and S. Gleyzes, A sensitive electrometer based on a Rydberg atom in a Schrödinger-cat state, *Nature (London)* **535**, 262 (2016).
- [6] U. Eichmann, T. Nubbemeyer, H. Rottke, and W. Sandner, Acceleration of neutral atoms in strong short-pulse laser fields, *Nature (London)* **461**, 1261 (2009).
- [7] S. D. Hogan, C. Seiler, and F. Merkt, Rydberg-State-Enabled Deceleration and Trapping of Cold Molecules, *Phys. Rev. Lett.* **103**, 123001 (2009).
- [8] S. Eilzer and U. Eichmann, Steering neutral atoms in strong laser fields, *J. Phys. B: At. Mol. Opt. Phys.* **47**, 204014 (2014).
- [9] R. E. Carley, E. Heesel, and H. H. Fielding, Femtosecond lasers in gas phase chemistry, *Chem. Soc. Rev.* **34**, 949 (2005).

- [10] H. Liu, Y. Q. Liu, L. B. Fu, G. G. Xin, D. F. Ye, J. Liu, X. T. He, Y. D. Yang, X. R. Liu, Y. K. Deng, C. Y. Wu, and Q. H. Gong, Low Yield of Near-Zero-Momentum Electrons and Partial Atomic Stabilization in Strong-Field Tunneling Ionization, *Phys. Rev. Lett.* **109**, 093001 (2012).
- [11] W. H. Xiong, J. W. Geng, J. Y. Tang, L. Y. Peng, and Q. H. Gong, Mechanisms of Below-Threshold Harmonic Generation in Atoms, *Phys. Rev. Lett.* **112**, 233001 (2014).
- [12] A. Talebpour, C. Y. Chien, and S. L. Chin, Population trapping in rare gases, *J. Phys. B: At. Mol. Opt. Phys.* **29**, 5725 (1996).
- [13] T. Nubbemeyer, K. Gorling, A. Saenz, U. Eichmann, and W. Sandner, Strong-Field Tunneling without Ionization, *Phys. Rev. Lett.* **101**, 233001 (2008).
- [14] B. Manschwetus, T. Nubbemeyer, K. Gorling, G. Steinmeyer, U. Eichmann, H. Rottke, and W. Sandner, Strong Laser Field Fragmentation of H_2 : Coulomb Explosion without Double Ionization, *Phys. Rev. Lett.* **102**, 113002 (2009).
- [15] T. Nubbemeyer, U. Eichmann, and W. Sandner, Excited neutral atomic fragments in the strong-field dissociation of N_2 molecules, *J. Phys. B: At. Mol. Opt. Phys.* **42**, 134010 (2009).
- [16] A. Azarm, S. Ramakrishna, A. Talebpour, S. Hosseini, Y. Teranishi, H. L. Xu, Y. Kamali, J. Bernhardt, S. H. Lin, T. Seideman, and S. L. Chin, Population trapping and rotational revival of N_2 molecules during filamentation of a femtosecond laser pulse in air, *J. Phys. B: At. Mol. Opt. Phys.* **43**, 235602 (2010).
- [17] A. Azarm, S. M. Sharifi, A. Sridharan, S. Hosseini, Q. Q. Wang, A. M. Popov, O. V. Tikhonova, E. A. Volkova, and S. L. Chin, Population trapping in Xe atoms, *J. Phys.: Conf. Ser.* **414**, 012015 (2013).
- [18] W. B. Zhang, Z. Q. Yu, X. C. Gong, J. P. Wang, P. F. Lu, H. Li, Q. Y. Song, Q. Y. Ji, K. Lin, J. Y. Ma, H. X. Li, F. H. Sun, J. J. Qiang, H. P. Zeng, F. He, and J. Wu, Visualizing and Steering Dissociative Frustrated Double Ionization of Hydrogen Molecules, *Phys. Rev. Lett.* **119**, 253202 (2017).
- [19] H. Zimmermann, S. Patchkovskii, M. Ivanov, and U. Eichmann, Unified Time and Frequency Picture of Ultrafast Atomic Excitation in Strong Laser Fields, *Phys. Rev. Lett.* **118**, 013003 (2017).
- [20] W. B. Zhang, H. Li, X. C. Gong, P. F. Lu, Q. Y. Song, Q. Y. Ji, K. Lin, J. Y. Ma, H. X. Li, F. H. Sun, J. J. Qiang, H. P. Zeng, and J. Wu, Tracking the electron recapture in dissociative frustrated double ionization of D_2 , *Phys. Rev. A* **98**, 013419 (2018).
- [21] S. Larimian, S. Erattupuzha, A. Baltuška, M. Kitzler-Zeiler, and X. H. Xie, Frustrated double ionization of argon atoms in strong laser fields, *Phys. Rev. Res.* **2**, 013021 (2020).
- [22] M. V. Fedorov and A. M. Movsesian, Field-induced effects of narrowing of photoelectron spectra and stabilisation of Rydberg atoms, *J. Phys. B: At. Mol. Opt. Phys.* **21**, L155 (1988).
- [23] M. V. Fedorov and M. Yu. Ivanov, Coherence and interference in a Rydberg atom in a strong laser field: excitation, ionization, and emission of light, *J. Opt. Soc. Am. B* **7**, 569 (1990).
- [24] A. M. Popov, O. V. Tikhonova, and E. A. Volkova, Low-frequency strong-field ionization and excitation of hydrogen atom, *Laser Phys.* **20**, 1028 (2010).
- [25] M. V. Fedorov, N. P. Poluektov, A. M. Popov, O. V. Tikhonova, V. Yu. Kharin, and E. A. Volkova, Interference stabilization revisited, *IEEE J. Sel. Top. Quantum Electron.* **18**, 42 (2012).
- [26] A. M. Popov, O. V. Tikhonova, and E. A. Volkova, Population trapping of excited atoms in strong chirped laser pulses, *J. Phys. B: At. Mol. Opt. Phys.* **47**, 204012 (2014).
- [27] N. I. Shvetsov-Shilovski, S. P. Goreslavski, S. V. Popruzhenko, and W. Becker, Capture into Rydberg states and momentum distributions of ionized electrons, *Laser Phys.* **19**, 1550 (2009).
- [28] B. B. Wang, X. F. Li, P. M. Fu, J. Chen, and J. Liu, Coulomb potential recapture effect in above-barrier ionization in laser pulses, *Chin. Phys. Lett.* **23**, 2729 (2006).
- [29] R. R. Freeman, P. H. Bucksbaum, H. Milchberg, S. Darack, D. Schumacher, and M. E. Geusic, Above-Threshold Ionization with Subpicosecond Laser Pulses, *Phys. Rev. Lett.* **59**, 1092 (1987).
- [30] E. A. Volkova, A. M. Popov, and O. V. Tikhonova, Ionization and stabilization of atoms in a high-intensity, low-frequency laser field, *J. Exp. Theor. Phys.* **113**, 394 (2011).
- [31] Q. Li, X.-M. Tong, T. Morishita, H. Wei, and C. D. Lin, Fine structures in the intensity dependence of excitation and ionization probabilities of hydrogen atoms in intense 800-nm laser pulses, *Phys. Rev. A* **89**, 023421 (2014).
- [32] S. L. Hu, X. L. Hao, H. Lv, M. Q. Liu, T. X. Yang, H. F. Xu, M. X. Jin, D. J. Ding, Q. G. Li, W. D. Li, W. Becker, and J. Chen, Quantum dynamics of atomic Rydberg excitation in strong laser fields, *Opt. Express* **27**, 31629 (2019).
- [33] M. Q. Liu, S. P. Xu, S. L. Hu, W. Becker, W. Quan, X. J. Liu, and J. Chen, Electron dynamics in laser-driven atoms near the continuum threshold, *Optica* **8**, 765 (2021).
- [34] S. Kim, J. Jin, Y.-J. Kim, I.-Y. Park, Y. Kim, and S.-W. Kim, High-harmonic generation by resonant plasmon field enhancement, *Nature (London)* **453**, 757 (2008).
- [35] M. F. Ciappina, J. Biegert, R. Quidant, and M. Lewenstein, High-order-harmonic generation from inhomogeneous fields, *Phys. Rev. A* **85**, 033828 (2012).
- [36] L. X. He, Z. Wang, Y. Li, Q. B. Zhang, P. F. Lan, and P. X. Lu, Wavelength dependence of high-order-harmonic yield in inhomogeneous fields, *Phys. Rev. A* **88**, 053404 (2013).
- [37] X. L. Ge, H. Du, Q. Wang, J. Guo, and X. S. Liu, Selection of quantum path in high-order harmonics and isolated sub-100 attosecond generation in few-cycle spatially inhomogeneous laser fields, *Chin. Phys. B* **24**, 023201 (2015).
- [38] A. Chacón, M. F. Ciappina, and M. Lewenstein, Double-electron recombination in high-order-harmonic generation driven by spatially inhomogeneous fields, *Phys. Rev. A* **94**, 043407 (2016).
- [39] H. Y. Zhong, J. Guo, W. Feng, P. C. Li, and X. S. Liu, Comparison of high harmonic generation and attosecond pulse from 3D hydrogen atom in three kinds of inhomogeneous fields, *Phys. Lett. A* **380**, 188 (2016).
- [40] I. N. Ansari, M. S. Mrudul, M. F. Ciappina, M. Lewenstein, and G. Dixit, Simultaneous control of harmonic yield and energy cutoff of high-order harmonic generation using seeded plasmonically enhanced fields, *Phys. Rev. A* **98**, 063406 (2018).
- [41] P. Rueda, F. Videla, E. Neyra, J. A. Pérez-Hernández, M. F. Ciappina, and G. A. Torchia, Above-threshold ionization driven by few-cycle spatially bounded inhomogeneous laser fields, *J. Phys. B: At. Mol. Opt. Phys.* **53**, 065403 (2020).
- [42] I. Yavuz, E. A. Bleda, Z. Altun, and T. Topcu, Generation of a broadband xuv continuum in high-order-harmonic generation

- by spatially inhomogeneous fields, *Phys. Rev. A* **85**, 013416 (2012).
- [43] M. F. Ciappina, J. A. Pérez-Hernández, T. Shaaran, J. Biegert, R. Quidant, and M. Lewenstein, Above-threshold ionization by few-cycle spatially inhomogeneous fields, *Phys. Rev. A* **86**, 023413 (2012).
- [44] Y. K. Chen, Y. M. Zhou, J. Tan, M. Li, W. Cao, and P. X. Lu, Photoelectron holography in strong-field tunneling ionization by a spatially inhomogeneous field, *Phys. Rev. A* **104**, 043107 (2021).
- [45] S. L. Hu, Z. X. Zhao, and T. Y. Shi, B-spline one-center method for molecular Hartree-Fock calculations, *Int. J. Quantum Chem.* **114**, 441 (2014).
- [46] H. Lv, W. L. Zuo, L. Zhao, H. F. Xu, M. X. Jin, D. J. Ding, S. L. Hu, and J. Chen, Comparative study on atomic and molecular Rydberg-state excitation in strong infrared laser fields, *Phys. Rev. A* **93**, 033415 (2016).
- [47] H. Bachau, E. Cormier, P. Decleva, J. E. Hansen, and F. Martín, Applications of B-splines in atomic and molecular physics, *Rep. Prog. Phys.* **64**, 1815 (2001).